sadasivans 27/12/11 13:30 TAJE_A_605801 (XML)

Australian Journal of Earth Sciences (2012) **00**, (1–16)

Australian paleo-stress fields and tectonic reactivation over the past 100 Ma

R. D. MÜLLER[1]*, S. DYKSTERHUIS[1,2] AND P. REY[1]

[1]*EarthByte Group, School of Geosciences, The University of Sydney, Madsen Building F09, NSW 2006, Australia.*
[2]*ExxonMobil, 12 Riverside Quay, Southbank, VIC 3006, Australia.*

Even though a multitude of observations suggest time-dependent regional tectonic reactivation of the Australian Plate, its large-scale intraplate stress field evolution remains largely unexplored. This arises because intraplate paleo-stress models are difficult to construct, and that observations of tectonic reactivation are often hard to date. However, because the Australian plate has undergone significant changes in plate boundary types and geometries since the Cretaceous, we argue that even simple models can provide some insights into the nature and timing of crustal reactivation through time. We present Australian intraplate stress models for key times from the Early Cretaceous to the present, and link them to geological observations for evaluating time-dependent fault reactivation. We focus on the effect time-dependent geometries of mid-ocean ridges, subduction zones and collisional plate boundaries around Australia have on basin evolution and fault reactivation through time by reconstructing tectonic plates, restoring plate boundary configurations, and modelling the effect of selected time-dependent plate driving forces on the intraplate stress field of a rheologically heterogeneous plate. We compare mapped fault reactivation histories with paleo-stress models via time-dependent fault slip tendency analysis employing Coulomb-Navier criteria to determine the likelihood of strain in a body of rock being accommodated by sliding along pre-existing planes of weakness. This allows us to reconstruct the dominant regional deformation regime (reverse, normal or strike-slip) through time. Our models illustrate how the complex interplay between juxtaposed weak and strong geological plate elements and changes in far-field plate boundary forces have caused intraplate orogenesis and/or tectonic reactivation in basins and fold belts throughout Australia.

KEY WORDS: paleo-stress, fault reactivation, plate tectonics, crustal deformation, Cretaceous-Recent, Cenozoic.

INTRODUCTION

Faults are a key aspect in many of Australia's sedimentary basins that have undergone significant reactivation resulting in the breaching of hydrocarbon traps. In particular, Oligocene collisional processes north of Australia (Cloetingh *et al.* 1992) and the Miocene separation of the Indo-Australian Plate into two distinct plates along a diffuse plate boundary (Royer & Chang 1991) have played an instrumental role in modifying the intra-plate stress field, resulting for instance in Miocene reactivation in the Timor Sea (O'Brian *et al.* 1996). The timing of Cenozoic tectonic events on the Northwest Shelf (NWS) compiled by Cloetingh *et al.* (1992) indicates a fundamental connection between plate tectonics, i.e. changes in plate motions and related in-plane stresses, and basin subsidence/uplift. As many basins of the Australian Northwest Shelf area have been subjected to a number of repeated extensional and compressional tectonic stages, controlling hydrocarbon migration in fault-controlled traps, understanding fault-trap charging and integrity requires some knowledge of paleo-stresses. Etheridge *et al.* (1991) pointed out that, in particular, steeply dipping strike-slip faults develop into wrench-reactivated transfer faults with associated structures that dominate traps in the Carnarvon, Bonaparte and Gippsland Basins. In central and eastern Australia, major reactivation of basin forming structures occurred in the early Late Cretaceous (*ca* 95 Ma, e.g. Hill 1994; Korsch *et al.* 2009) when plate motion to the east slowed down before to change towards a northerly direction.

While modelling of the contemporary maximum horizontal stress (σ_H) regime is useful for improving our understanding of the driving forces of plate tectonics as well as for the planning of deviated drilling during hydrocarbon production, information concerning paleo-stress regimes allows for the creation of predictive frameworks for fault reactivation through time. Compilation of stress data under the auspices of the World Stress Map project in the early 1980s (Zoback 1992) showed σ_H orientations over most continental areas are parallel to the direction of absolute plate motion, leading to the hypothesis that σ_H orientations are the product of dominant plate driving forces acting

*Corresponding author: dietmar.muller@sydney.edu.au

ISSN 0812-0099 print/ISSN 1440-0952 online
http://dx.doi.org/10.1080/08120099.2011.605801

along plate boundaries (Zoback 1992). Orientations of σ_H over various portions of the Indo-Australian Plate, Eurasia and South America, however, have been found to be more complex and are not parallel to absolute plate motion trajectories, indicating that plate boundary forces alone are not enough to understand intra-plate stress (Heidbach *et al.* 2007). Here we use the Australian paleo-stress model presented by Dyksterhuis & Müller (2008), utilising provinces within the Australian continent with differing rigidity, and focus on a comparison with geological observations from a number of different basins across the continent, particularly on the Northwest Shelf of Australia. If the main features of these paleo-stress maps can be validated in those areas where reliable indicators for tectonic reactivation are present, then the maps have the potential to be used in a predictive sense in areas with sparse data.

METHODOLOGY

We map Australian Cenozoic intraplate stress evolution based on Dyksterhuis & Müller (2008), with one additional but more uncertain model for the Cretaceous (100 Ma), using a methodology described in detail previously (Dyksterhuis & Müller 2004, 2008; Dyksterhuis *et al.* 2005a, b). To understand the effect of time-dependent geometries of mid-ocean ridges, subduction zones and collisional plate boundaries on the reactivation of Australia's main tectonic elements (Figure 1) through time, we reconstruct tectonic plates, including ocean floor which has now entirely vanished, restore plate boundary configurations (Figure 2), and model the effect of selected time-dependent plate driving forces on the intraplate stress field. We create a two dimensional, elastic, plane stress finite element model of the (Indo-) Australian Plate that distinguishes cratons, fold belts, basins (Figure 1), and ocean crust in terms of their relative differences in mechanical stiffness. The numerical model setup and parameters used can be found in Dyksterhuis & Müller (2008). Orientations of modelled present-day maximum horizontal stress directions (σ_H) agree well with observed directions contained in the Australian Stress Map Database, with a mean residual misfit of $\sim 12^\circ$.

In order to compare Australia-wide paleo-stress models based on those described in Dyksterhuis & Müller (2008) with observations from key basins, we make use of slip-tendency diagrams, based on a Matlab script developed by U. Theune and M. Gölke (http://www-geo.phys.ualberta.ca/~utheune/SlipTendency/slip_html.html), using a methodology described in Morris *et al.* (1996). Slip Tendency (T) is defined as the ratio of shear (τ) to normal stress (σ_n) normalised by the coefficient of friction (μ):

$$T = \tau/(\mu \times \sigma_n)$$

The value of the slip tendency for a fault segment is a measure for its likelihood to fail under the given stress

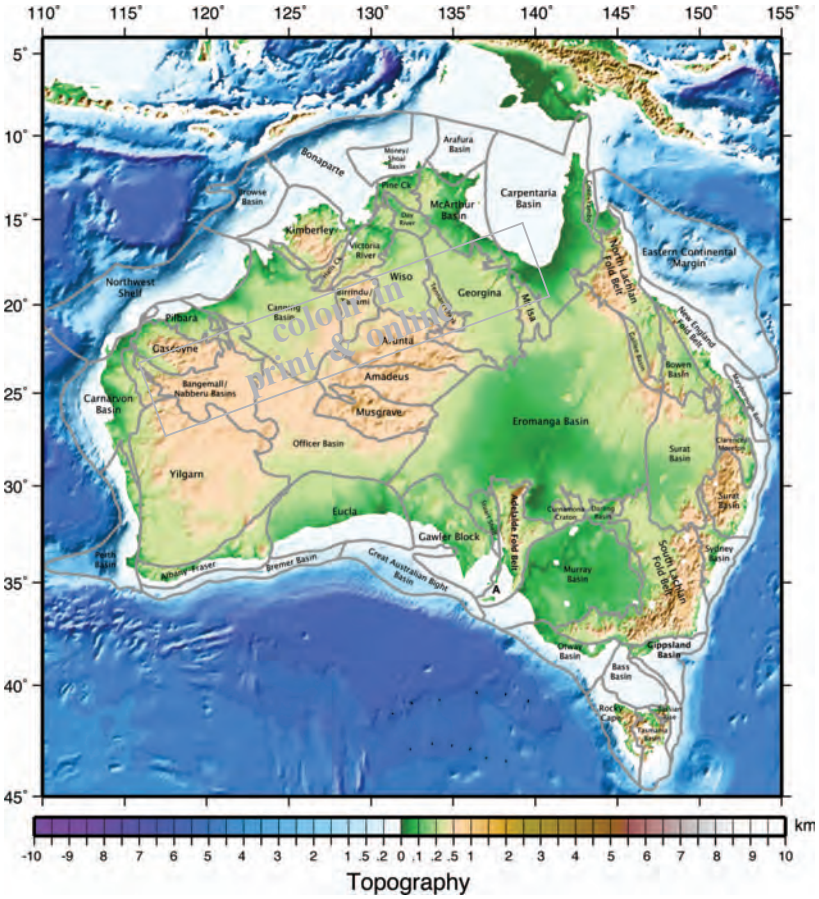

Figure 1 Topography/bathymetry map of Australia with model rheological provinces shown by grey outlines (relative strengths listed in Dyksterhuis & Müller 2008).

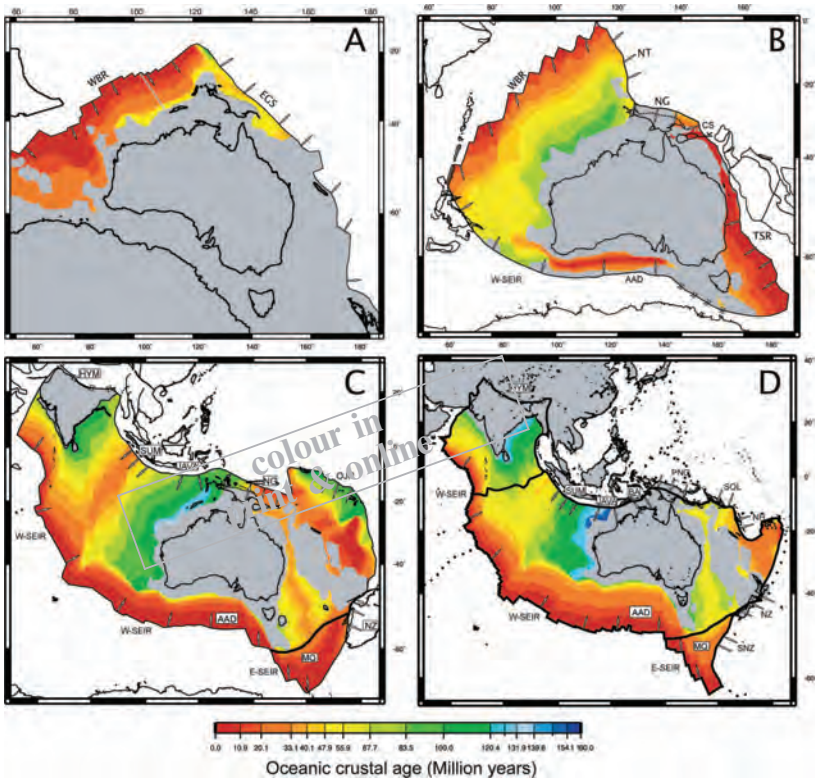

Figure 2 Indo-Australian Plate with age-area distribution of the oceanic crust (coloured) and location of plate driving forces applied to a model of the (Indo-) Australian Plate (A) 100 Ma, (B) 55 Ma, (C) 25 to 11 Ma and (D) 11 to 0 Ma. HYM = Himalayas (fixed boundary), SUM = Sumatra Trench, JAVA = Java Trench, BA = Banda Arc, PNG = Papua New Guinea, SOL = Solomon Trench, NH = New Hebrides, NZ = New Zealand, SNZ = Australian/Pacific plate margin south of New Zealand, AAD = Australia Antarctic Discordance, MQ = Macquarie Plate, OJP = Ontong Java Plateau, CS = Coral Sea, W-SEIR = Western Southeast Indian Ridge, E-SEIR = Eastern Southeast Indian Ridge WBR = Wharton Basin Ridge, NG = New Guinea Margin, NT = Northern Trench, TSR = Tasman Sea Ridge, EGS = East Gondwanaland Subduction Zone. Note that force arrows are not drawn to scale. Projections used for transforming points of latitude and longitude along the plate margins to and from a Cartesian reference frame for use in ABAQUS are listed in Appendix 1.

field. A small value of T indicates stable faults, whereas values close to one indicate critically stressed faults. For a pre-existing fault to be reactivated, the shear stress (τ) on the fault must exceed a certain critical value (τc) defined as:

$$\tau c \geq \mu \times \sigma_n$$

where μ is the coefficient of friction, and σ_n is the normal stress acting on the fault plane.

Based on the orientation and magnitude of the modelled far-field maximum horizontal stress as well as the magnitude of the minimum horizontal stress (Table 1) and fault properties (i.e. coefficient of friction and cohesion) the Matlab code used here calculates the slip tendency for all possible fault plane orientations. The strike of modelled fault planes is varied between 0 and 360°E, and their dip is varied between 0° and 90°, both increasing in steps of 2°, so that 8326 fault plane orientations are analysed for each case. The computed slip tendencies are plotted as coloured points on a stereo net. The user can then superimpose the orientation of a known, existing fault or fault system for a given area to assess the likelihood for reactivation under the modelled stress regime.

Reactivation and inversion of steeply dipping (≥60°) faults occurs over the Australian continent at various times. Analogue modelling work by Brun & Nalpas (1996) demonstrated that transpressional reactivation (strike-slip reactivation with a component of reverse motion) occurs along steeply dipping faults when the direction of σ_H is oriented at an angle less than 45° to the strike of the fault. Regional stress regimes are therefore more likely to reactivate steeply dipping to vertical pre-existing weaknesses where they are oblique (less than 45°) to the structural fabric of a given region.

RESULTS

Modelled present-day σ_H directions can be directly compared with measured σ_H directions in the Australian Stress Map database to validate the model. The validation process for the paleo-stress models is not straightforward given the sparseness of data for direct comparison. The most useful information for this purpose is recorded in the geological history as deformation events through time, via successively reactivated generations of faults (normal, reverse, strike-slip) and folds. In order to validate our paleo-stress models, we have reviewed the deformation record of numerous

Table 1 Magnitude and azimuth of modelled maximum horizontal stress (σ_H) and minimum horizontal stress (σ_h) averaged over a small rectangular area indicated by present-day lat./long. coordinates in the table for different time periods.

Time period	Azimuth	σ_H (MPa)	σ_h (MPa)	Figure 3 key
NW Shelf (Browse)	118/123/-16/-13 (W/E/S/N)			
6–0 Ma	70	56	–54	A4
11–6 Ma	67	50	–57	A3
23–11 Ma	117	69	–45	A2
ca 55 Ma	112	6	1	A1
Flinders	138/140/-34/-30 (W/E/S/N)			
6–0 Ma	106	9	2	B4
11–6 Ma	69	6	3	B3
23–11 Ma	118	22	–9	B2
ca 55 Ma	85	14	2	B1
Gippsland	146/149/-39/-38 (W/E/S/N)			
6–0 Ma	129	8	1	C4
11–6 Ma	90	6	3	C3
23–11 Ma	135	25	2	C2
ca 55 Ma	87	1	–0.1	C1

Magnitudes of modelled σ_H and σ_h represent the differential stress from a lithostatic reference state of 20 MPa, a coefficient of friction of 0.6 and a cohesion of 0 MPa (cohesionless faults). 'Azimuth' refers to azimuth of the maximum horizontal stress (σ_H).

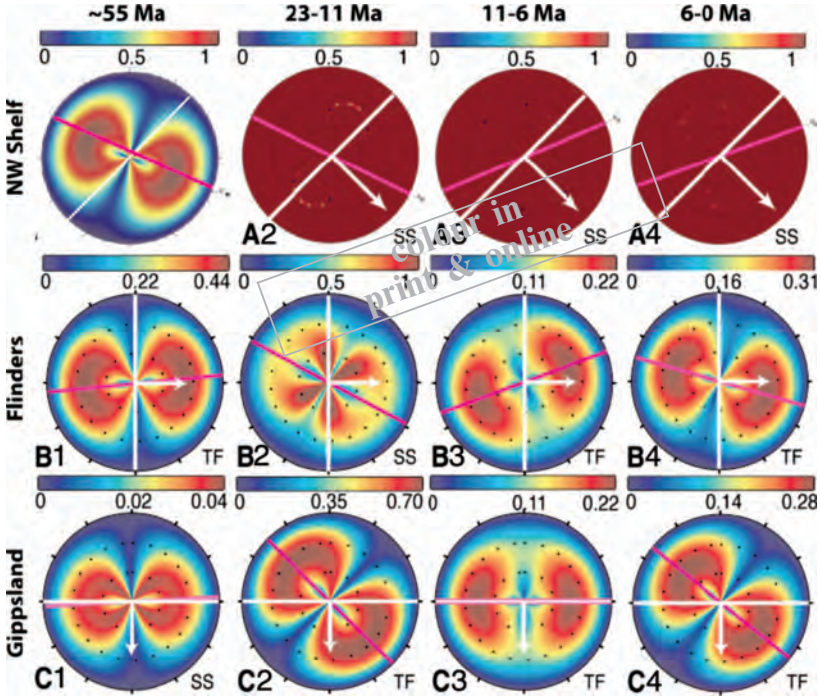

Figure 3 Equal area lower hemisphere stereonets indicating slip tendency, with hotter colours indicating greater likelihood slip to occur for particular combinations of dip and strike of a given fault. Uniformly red colours in diagrams A2–4, indicate differential stress saturation, for the Miocene to present Northwest Shelf result from very large differences in modelled maximum and minimum horizontal stresses. However, it needs to be kept in mind that our models are simplified, and do not take into account depth-dependence of fault reactivation, mantle processes or plate flexure—therefore these models become less robust close to plate boundaries. Especially the modelled minimum horizontal stresses here are likely too low and may be in error, reflecting oversimplications in our model in regions close to plate boundaries. The dominant stress regime at these times (strike slip) is nevertheless interpreted to be the most likely regime with faults oriented at ~45° to the maximum horizontal stress orientation, the most favourable orientation for strike-slip reactivation. Planes are represented on the stereonets by a single point placed at 90° to the strike of the plane with the dip of the plane indicated by the pole's proximity to the centre (the large black stippled circle indicates a dip of 60°, the small black stippled circle indicates a dip of 30° with the centre representing a dip of 0°). Slip tendency graphs are computed for a lithostatic stress state of 20 MPa, a coefficient of friction of 0.6 and a cohesion of 0 MPa (cohesionless faults). Slip tendency graphs for three regions at various modelled times are shown: North West Shelf (Browse Basin) (A1–A4) [(A1) 55 Ma, (A2) 23 to 11 Ma, (A3) 11 to 6 Ma and (A4) 6 to 0 Ma], the Flinders Ranges (B1–B4) [(B1) 55 Ma, (B2) 23 to 11 Ma, (B3) 11 to 6 Ma and (B4) 6 to 0 Ma] and the Gippsland Basin (C1–C4) [(C1) 55 Ma, (C2) 23 to 11 Ma, (C3) 11 to 6 Ma and (C4) 6 to 0 Ma]. See Table 1 for mean σ_H azimuth and principle stress magnitudes for individual time periods. The white line indicates the strike of the structural fabric for the region with the white arrow indicating the pole to the plane indicating general dip of faults. The modelled maximum horizontal stress orientation is overlain in pink. Andersonian stress regime style is indicated by text at the lower right of each stereonet where NF = normal faulting, TF = thrust faulting and SS = strike-slip faulting.

sedimentary basins in the Northwest Australian Shelf, Gippsland Basin, Flinders Ranges and eastern Australia to test both the spatial and temporal fit of the modelled σ_H regime for the modelled time periods.

Tectonic reactivation history of the Northwest Shelf of Australia

The Northwest Australian Shelf (NWS) (Figure 4) has a general northeast-trending structural fabric inherited from Late Permian rifting (Keep *et al.* 1998). Reactivation and inversion of older structures as well as generation of anticlines within the basins of the NWS occurred through time. The Browse Basin holds two large Miocene inversion structures, the Lombardina and Lyner structures, interpreted to be transpressional anticlines (Figure 5) that continued to grow throughout the Late Miocene (Keep *et al.* 1998). Marked reactivation occurs dominantly on steep faults, with associated flower-type structures with significant inversion. Formation of transpressional anticlines is limited to one or two major faults with strain strongly partitioned along a few major faults (Keep *et al.* 1998).

There is a marked change in structural orientation on the NWS in the Carnarvon Basin from a northeast orientation in the north Carnarvon (Dampier sub-basin) to a north-northeast orientation in the south (Exmouth Sub-Basin) with significant concentration of structural inversion (Symonds & Cameron 1977). Faulting in the Carnarvon Terrace (a geographic term for the portion of the offshore Carnarvon Basin south of the Cape Range Transform Fault) during the Middle to Late Cretaceous is restricted to northeast-trending subvertical faults, which display a wrench reactivation with left-lateral sense of movement (indicative of a more north–south oriented maximum horizontal stress direction) (Baillie & Jacobson 1995). During the Miocene, with some activity into the present day, wrench reactivation of northeast-trending subvertical faults is apparent (Müller *et al.* 2002) with a right lateral sense of movement (indicative of a more east–west-oriented maximum horizontal stress direction). There are numerous Miocene inversion structures in the basin, with strain mainly partitioned along the Rough Range and Learmouth faults (Longley *et al.* 2002).

The Exmouth Sub-basin experienced at least two phases of uplift and erosion during the Cretaceous and inversion and tilting in the Paleogene–Neogene (Longley *et al.* 2002). The Barrow Sub-basin just northeast, however, did not experience this reactivation. In the Valanginian (137 Ma) the east–west-trending Ningaloo Arch was uplifted in the Exmouth Sub-Basin (Struckmeyer *et al.* 1998). Uplift occurred along the west-northwest-trending Novara Arch in the Santonian (84 Ma) in the Exmouth Sub-Basin, with intense extension along north-northeast to south-southwest-trending normal faults associated with this uplift, reactivating some Triassic/Jurassic faults (Struckmeyer *et al.* 1998).

Overview of Southeast Australian Deformation History

The Flinders Ranges (Figure 6), along with the Mount Lofty Ranges, are bounded by north–south to northeast–southwest-trending, moderately (40°–45°) dipping fault scarps that demonstrate deformation during the Neogene (Sandiford 2003; Celerier *et al.* 2005; Quigley *et al.* 2006). Exposures of range-bounding fault scarps reflect reverse reactivation (Sandiford 2003) while faults in the range interior are dominantly strike-slip movement (Clark & Leonard 2003). In addition, significant Neogene–Quaternary deformation and exhumation has occurred to the east

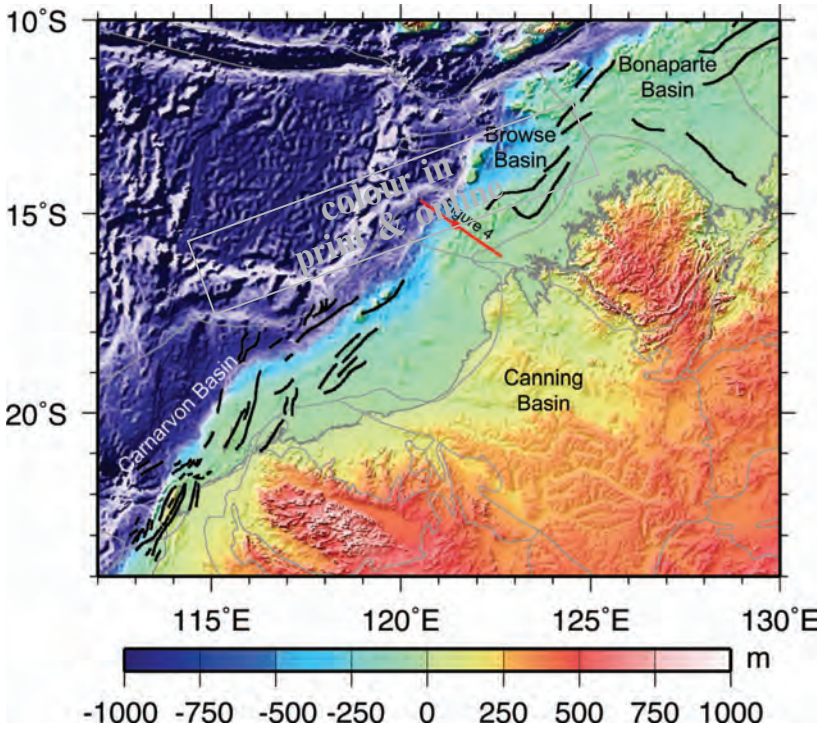

Figure 4 Major elements of the Northwest Australian Shelf showing main basins and main structural trends (black lines). Location of seismic line shown in Figure 5 indicated by red line.

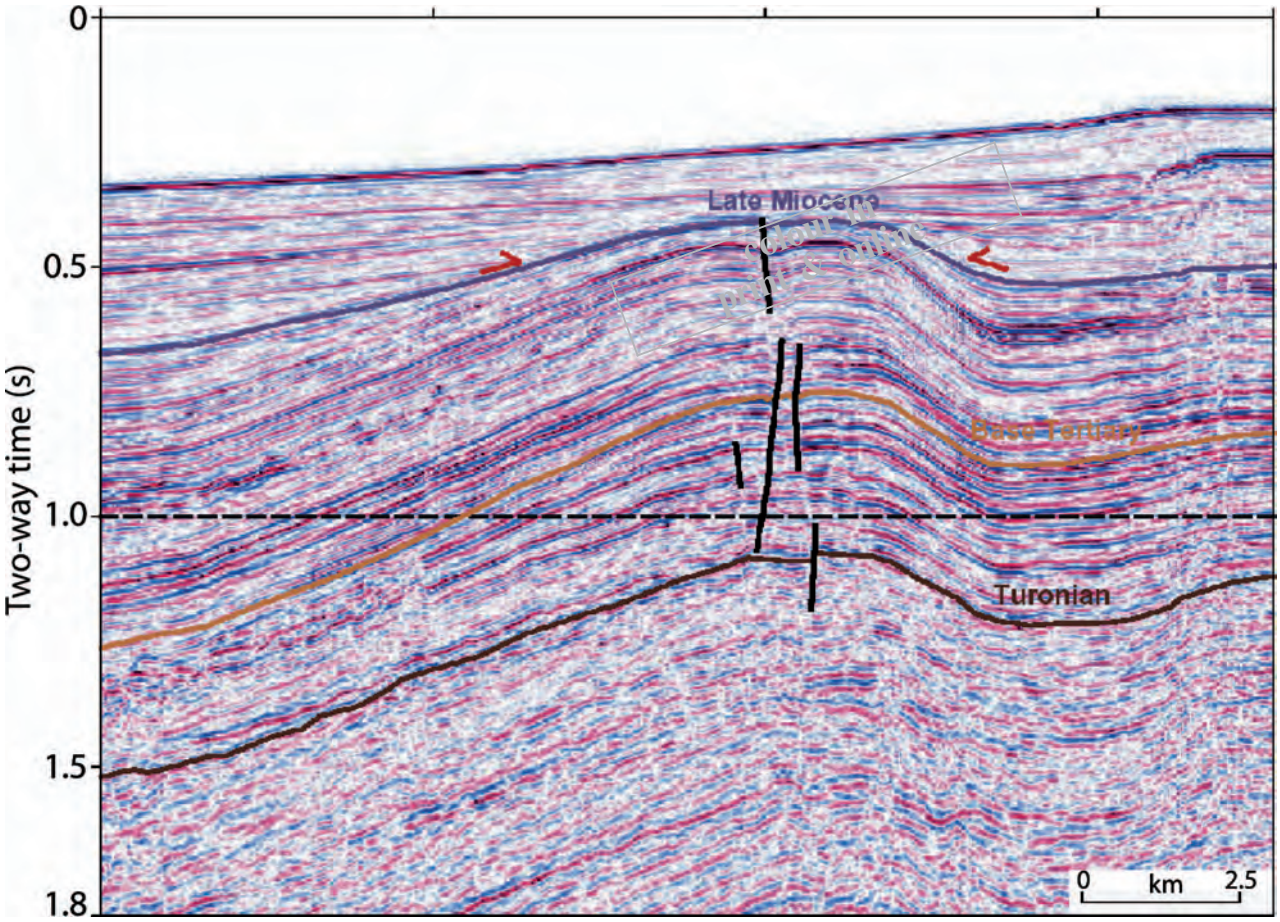

Figure 5 Miocene inversion structure over the Lombardina structure, Browse Basin, Northwest Shelf, AGSO seismic line 175/03 (modified from Struckmeyer *et al.* 1998, where a detailed interpretation of this structure can be found).

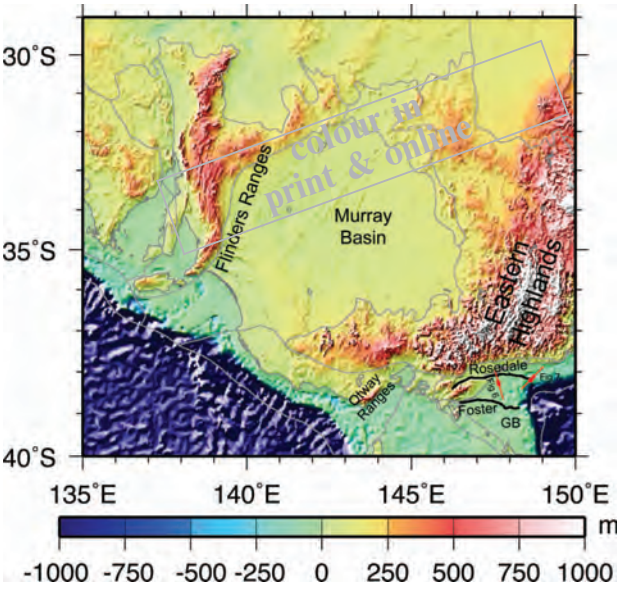

Figure 6 Relief map of the Flinders Ranges and the Gippsland Basin showing major faults and locations of seismic lines.

in the Gippsland Basin in South Eastern Australia (Dickinson *et al.* 2001), located hundreds of kilometres from the nearest plate margin. During the Oligocene, broad, low-relief northeast-trending anticlines were formed (Figure 7), while during the Miocene reverse reactivation of the east–west-trending margin normal Rosedale and Foster fault systems occurred (Figure 8) with up to 1 km of uplift (Dickinson *et al.* 2001).

Early Late Cretaceous Tectonic Inversion in Central and eastern Australia

In the Cretaceous, eastern Australia, then part of Gondwana's Pacific margin, was overriding a long-lived west dipping subduction zone. A succession of previous extensional events led to the formation of foreland sedimentary basins (Figure 1) including the Cooper and Simpson Basins (Permo-Carboniferous to Triassic), Bowen and Gunnedah Basins (Early Permian to Middle Triassic), Eromanga and Surat Basins (Early Jurassic to Early Cretaceous). These basins were inverted during contractional events, first in the Late Permian to Middle Triassic (New England Orogen) and later during the early Late Cretaceous at *ca* 95 Ma (Hill 1994; Korsch *et al.* 2009). During the latter, the switch from extension to contraction lead to uplift, erosion and deep weathering, folding and reactivation of northeasterly to northerly trending planar faults such as the Tamworth thrust (Glen & Brown 1993; Woodward 1995), the Moonie thrust; and further north the northeast-dipping Jellinbah thrust zone (Hobbs 1985; Korsch *et al.* 2009). Some reactivation led to the formation of hydrocarbon traps

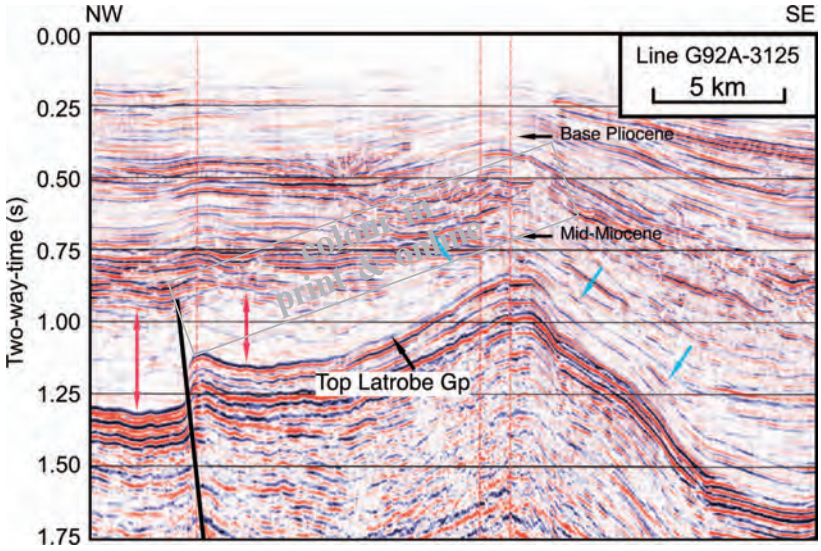

Figure 7 Seismic line G92A-3125 (see Figure 5 for location) offshore Gippsland Basin. Early Miocene sediments onlap (blue arrows) the deeper structure, indicating deformation within the Oligocene–Early Miocene. Onlapping reflectors, stratigraphic thinning and folding higher in the section indicate that deformation continued into the Plio-Pleistocene. Different stratigraphic thicknesses on either side of the reverse fault (red arrows) indicate fault movement within the Oligocene–Early Miocene (modified from Dickinson *et al.* 2001).

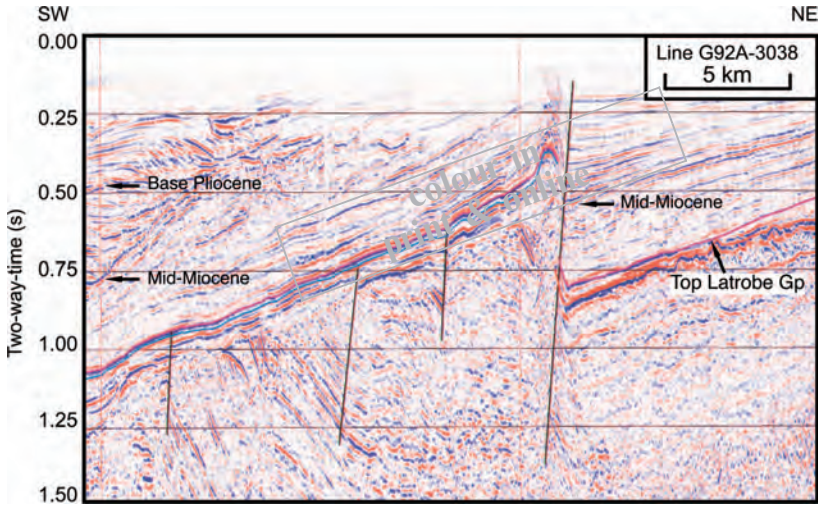

Figure 8 Seismic line G92A-3038 offshore Gippsland (see Figure 5 for location) showing relatively young (post-Middle Miocene) reverse movement on the Rosedale Fault System (modified from Dickinson *et al.* 2001).

in a number of Australian Basins including the Cooper Basin (Alexander & Jensen-Schmidt 1996).

The tectonic inversion in the early Late Cretaceous can be related to a major plate re-organisation. Paleogeographic reconstructions show that from 135 to 100 Ma ago, East Gondwana moved eastwards (Rey & Müller 2010), slowing between 115 and 100 Ma ago. Tectonic inversion in central and eastern Australia occurred when Gondwana stopped its eastward motion around 100 Ma, leading to extensional collapse of the Zealandia Cordillera orogen built along Gondwana's Pacific margin (Tulloch *et al.* 2006), in turn causing a period of coeval compression landward of the mountain belt (Rey & Müller 2010). Much later, some time during the Oligocene or Early Miocene silcrete caps were folded in central and eastern Australia (Alley 1998). This event may be linked to the Australia–India collision.

Modelling Results

CRETACEOUS (*CA* 100 MA)

In addition to the paleo-stress time slices discussed by Dyksterhuis & Müller (2008), we present one tentative model for the Cretaceous. During the Cretaceous, following Greater India–Australia break-up at *ca* 132 Ma, the Australian intraplate stress field was dominated by ridge push from the now subducted northern Wharton Basin Ridge in the Neo-Tethys Ocean (Figure 2A). Modelled σ_H directions for the Cretaceous (Figure 9) generally trend north–south over the entire continent. However, we regard the details in this model as substantially more uncertain than our Cenozoic models, and mainly include it to demonstrate the overall difference between the Cretaceous and the Eocene stress fields. With an average azimuth of roughly 60° to the main structural fabric in the Browse Basin, the orientation of σ_H directions is not oblique enough to cause any significant reverse reactivation or inversion of pre-existing northeast-trending structures, though strike-slip reactivation is possible. We do not regard the modelled stress directions in central and eastern Australia in this model as well constrained at this time, because mantle-driven forces may have played a large role (Matthews *et al.* 2011) relative to plate boundary forces at that time, in modulating the regional paleo-stress field.

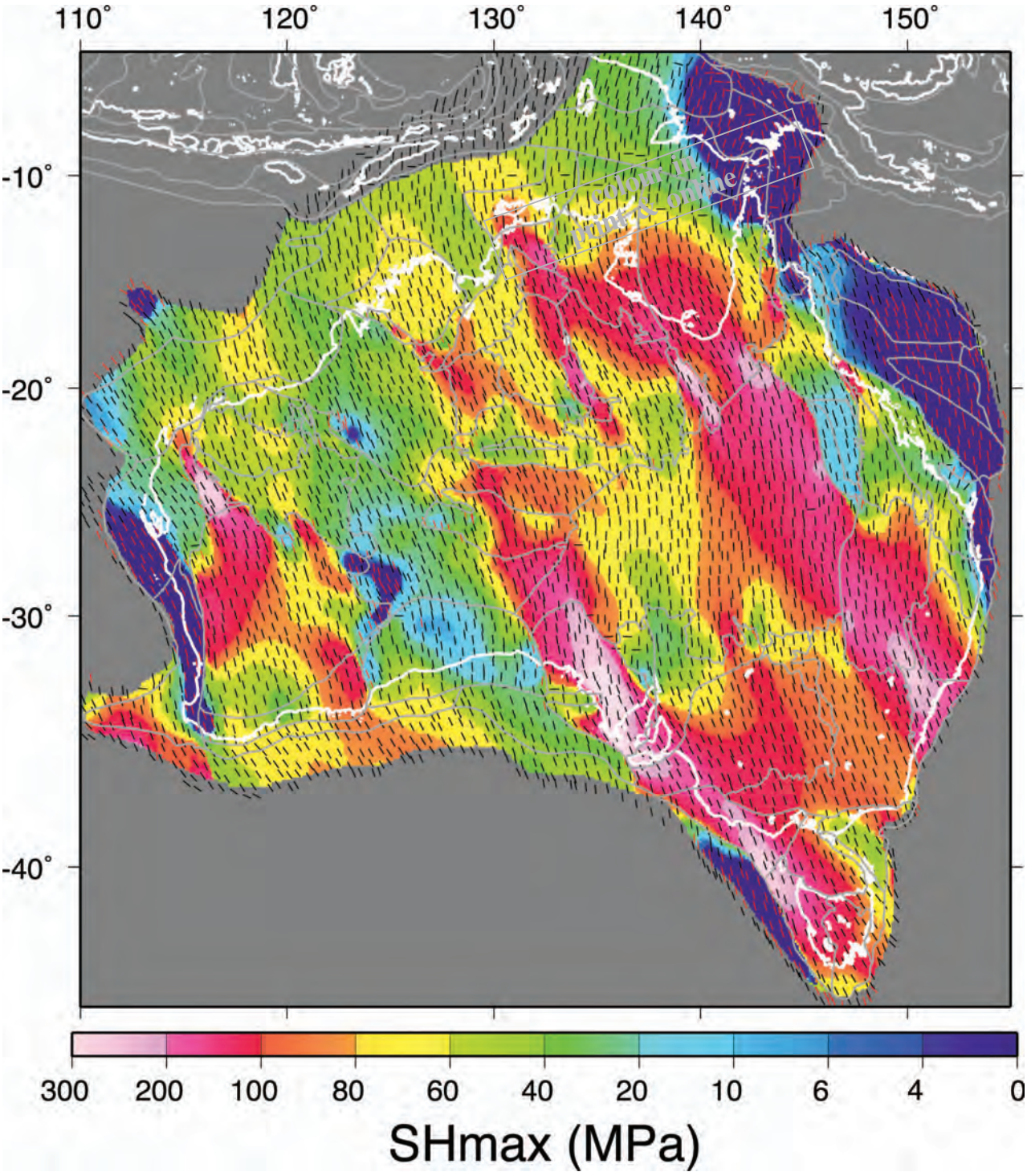

Figure 9 Modelled maximum horizontal stress for the Cretaceous (*ca* 100 Ma). Stress magnitude units are in MPa.

EARLY LATE CRETACEOUS TO EOCENE (*CA* 95–55 MA)

The Australian stress field is believed to have changed dramatically in the early Late Cretaceous (*ca* < 95 Ma) due to the establishment of plate driving forces from mid-ocean ridges to the east and south of Australia (Gaina & Müller 2007) (Figure 2B). Modelled σ_H magnitudes over Australia for the Eocene are relatively low at this time (Figure 10), with σ_H orientations now trending generally west-northwest over the NWS, and we propose that this tectonic regime was established at *ca* 95–90 Ma when a mid-ocean ridge was developing east of Australia. Reactivation of the northeast-trending structural fabric on the NWS at this time is most likely in a strike-slip regime (Figure 3A1). The northeast-trending modelled σ_H orientations on the Exmouth Plateau are compatible with the formation of northeast-trending anticlines, however, modelled σ_H magnitudes at this time are low, suggesting that folding may be unlikely.

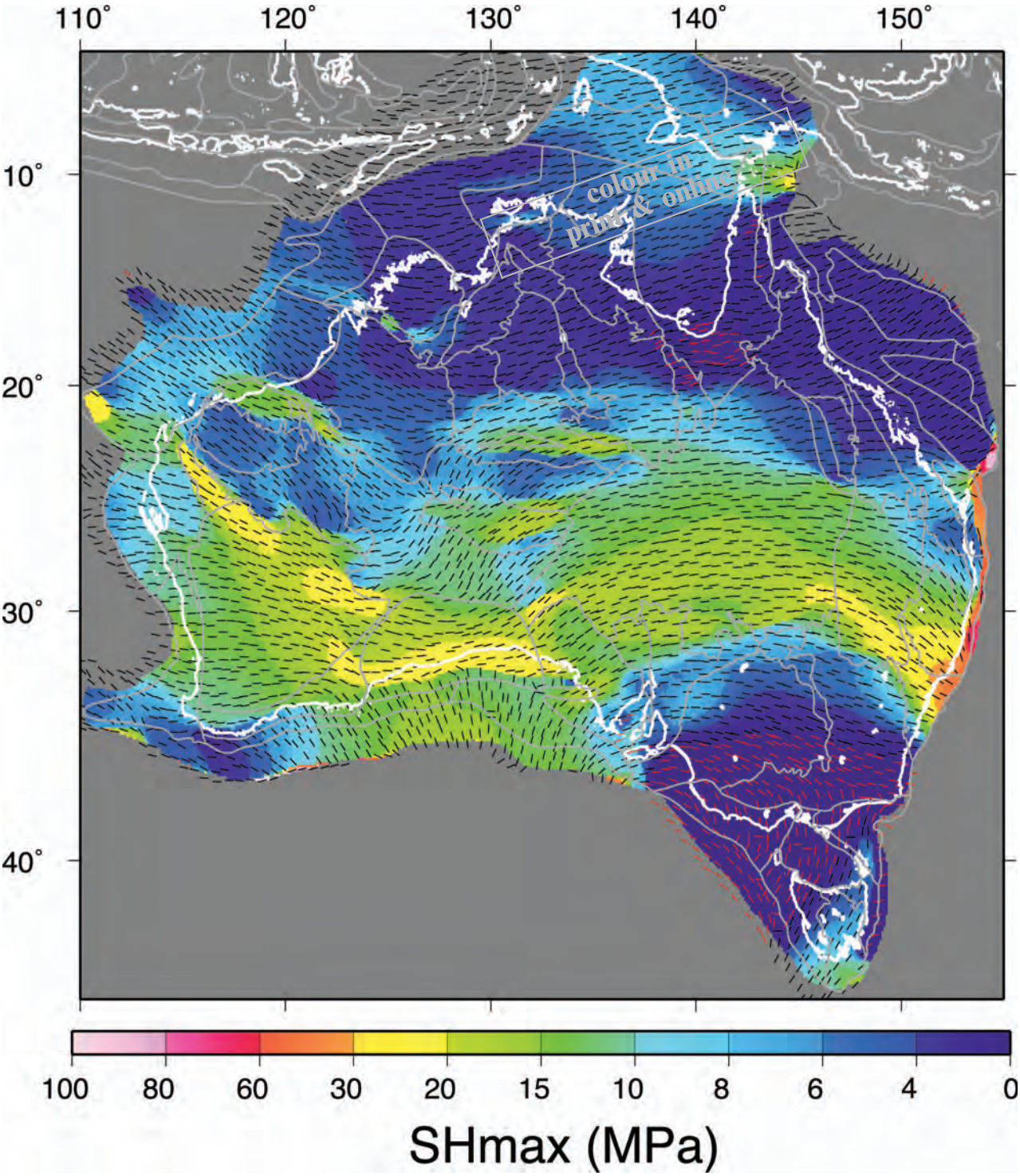

Figure 10 Modelled maximum horizontal stress for the Eocene (*ca* 55 Ma). Stress magnitude units are in MPa.

Modelled σ_H directions rotate to a roughly east–west orientation in the Flinders Ranges (Figure 10), central and eastern Australia, approximately orthogonal to the general north–south trending pre-existing fault fabric (Figure 3B1). In the Flinders Ranges, this is associated with a dramatic change in strain regime from strike-slip to reverse, while in central and eastern Australia the new stress regime explains the tectonic inversion of north–south trending normal faults. Slip tendency graphs (Figure 3B1) indicate east–west σ_H directions to be optimally orientated for reverse reactivation of the moderately dipping faults at shallow depths (Sandiford 2003). This suggests an Early Eocene onset of the Sprigg's Orogeny via reactivation of pre-existing faults (Dyksterhuis & Müller 2008). Evidence from apatite fission track analysis indicates that regional cooling of up to 60°C and uplift occurred in the Flinders Ranges during the Eocene (Mitchell *et al.* 2002), accompanied by an increase in sedimentation rates into surrounding

basins, supporting our model. Modelled σ_H magnitudes in the Gippsland Basin at *ca* 55 Ma show the region to be marginally in the strike-slip tectonic stress regime (Figure 3C1). Modelled stress magnitudes are very low, however, and other portions of southeast Australia appear to be in an extensional tectonic stress regime (Figure 10). This is supported the observation that extensional tectonism prevailed in the Gippsland Basin until the Early Eocene (Johnstone *et al.* 2001; Sandiford *et al.* 2004) with a compressional tectonic regime not becoming dominant until after the cessation of seafloor spreading in the Tasman Sea at *ca* 52 Ma (Bernecker *et al.* 2006).

A significant basin-forming event occurred along the east coast of Queensland in the Middle to Late Eocene, where a series of en-echelon graben and half-graben basins formed striking north-northwest (Gibson 1989). These basins host oil shales which have been explored since 1980 for hydrocarbons (McConnochie & Henstridge 1985). Our Eocene model shows extremely small-magnitude maximum horizontal stresses (Figure 10), bordering on an extensional regime, in qualitative agreement with the Eocene change in stress regime indicated by graben formation in East Queensland. Our modelled horizontal maximum stress directions are not oriented parallel to the strike of the grabens, as would be expected. This may be a consequence of uncertainties in the distribution of relatively weak and strong lithospheric elements in the region.

EARLY–MIDDLE MIOCENE (23–11 MA)

The σ_H magnitudes increase in amplitude over the NWS in the Early Miocene model (Figure 11) while σ_H orientations remain broadly similar to those during the Eocene, trending generally northwest on the NWS. Orientations of modelled σ_H directions remain northwest-trending in the Exmouth Plateau area between the Eocene and Early Miocene, however, the amplitude of the modelled σ_H magnitudes increases between the two time periods, suggesting that the formation of the northeast-trending antliclines (Symonds *et al.* 1994) occurred more likely between *ca* 55 to *ca* 23 Ma. This corresponds to a time period when spreading in the Tasman Sea ceased at *ca* 52 Ma, followed by a cessation of spreading in the Wharton Basin at *ca* 42 Ma (Krishna *et al.* 1995). The hard collision between India and Eurasia was likely initiated at *ca* 34 Ma (Aitchison *et al.* 2007), paired with the initiation of mountain building along Australia's eastern plate boundary along the Alpine Fault at *ca* 25 Ma (Kamp & Fitzgerald 1987). Together, these severely altered boundary forces established a stress regime in the Miocene dominated by ridge push south of Australia and increased resisting forces north of India and east of Australia, raising compressive stress magnitudes on the NWS severely in the Miocene compared with older model times, in agreement with structural observations indicating widespread Neogene tectonic reactivation in the Timor Sea (Shuster *et al.* 1998).

Modelled σ_H directions in the Flinders Ranges trend northwest in the Early to Middle Miocene. Magnitudes of modelled σ_H indicate a moderate likelihood of strike-slip reactivation of pre-existing faults at this time, with reverse reactivation of range bounding faults less likely compared with 55 Ma or the present day (Figure 3B2), suggesting a period of quiescence in the Flinders Ranges during the Early to Middle Miocene (Dyksterhuis & Müller 2008).

Modelled σ_H magnitudes in the Gippsland Basin were greatest in the Early to Middle Miocene with modelled σ_H directions trending southeast with a mean azimuth of 134°. A reverse faulting stress regime was extant and reactivation of steeply dipping, east–west-trending faults in the region, is interpreted to be moderately to highly likely (Figure 3C2). These results are consistent with observations that show compression along northeast–southwest-trending anticlines peaking during the Middle Miocene (Dickinson *et al.* 2001; Bernecker *et al.* 2006) with contemporaneous transpressional reactivation of east–west-trending faults (Dickinson *et al.* 2001).

The increase in modelled stress magnitudes in much of the Eromanga Basin in the Early Miocene is likely related to a period of broad-wavelength folding and faulting, observed in Cretaceous sediments in northeastern South Australia at various localities along the edge of the Simpson Desert and in the southwest Queensland portion of the Eromanga Basin (Sprigg 1963; Wopfner 1974). In addition, Gregory *et al.* (1967) and Senior *et al.* (1968) mapped about 40 equivalent anticlines in the southwest Queensland portion of the Eromanga Basin, based on the deformation of a previously formed silcrete surface, marking an originally flat-lying unconformity (Sprigg 1963). The associated fold axes are approximately NE–SW oriented and the fold wavelengths are up to around 50 km and larger with amplitudes of about 20 to 200 m (Sprigg 1986). Mavromatidis (2006) mapped a maximum uplift of 180 m associated with this deformation period. Finlayson & Leven (1988) and Wopfner (1978) estimated the timing of the deformation as Eogene/Oligocene–Early Miocene, in broad agreement with our model results.

LATE MIOCENE (11–6 MA)

The modelled σ_H regime (Figure 12) changes considerably at this time with the onset of collision at the Papua New Guinea margin (Hall 2002). This oblique collision is expressed by Miocene–Recent anomalous subsidence in the Cartier Trough and the Malita Graben, likely related to reactivation of rift structures by sinistral shear. Other structures in the Timor Sea have been inverted by left-lateral shear at confining bends of faults (Shuster *et al.* 1998). While previous models showed consistent trends for σ_H directions over the entire NWS, in the Late Miocene σ_H orientations rotate in a clockwise direction from east–west in the Carnarvon Basin to northeast in the Timor Sea. The mean σ_H orientation of 67° in the Browse Basin at this time indicates that transpressional reactivation of northeast-trending faults is likely (Figure 3A3). The documented right-lateral sense of movement on the faults at this time (Etheridge *et al.* 1991) agrees well with the general east–west trend of the modelled σ_H directions.

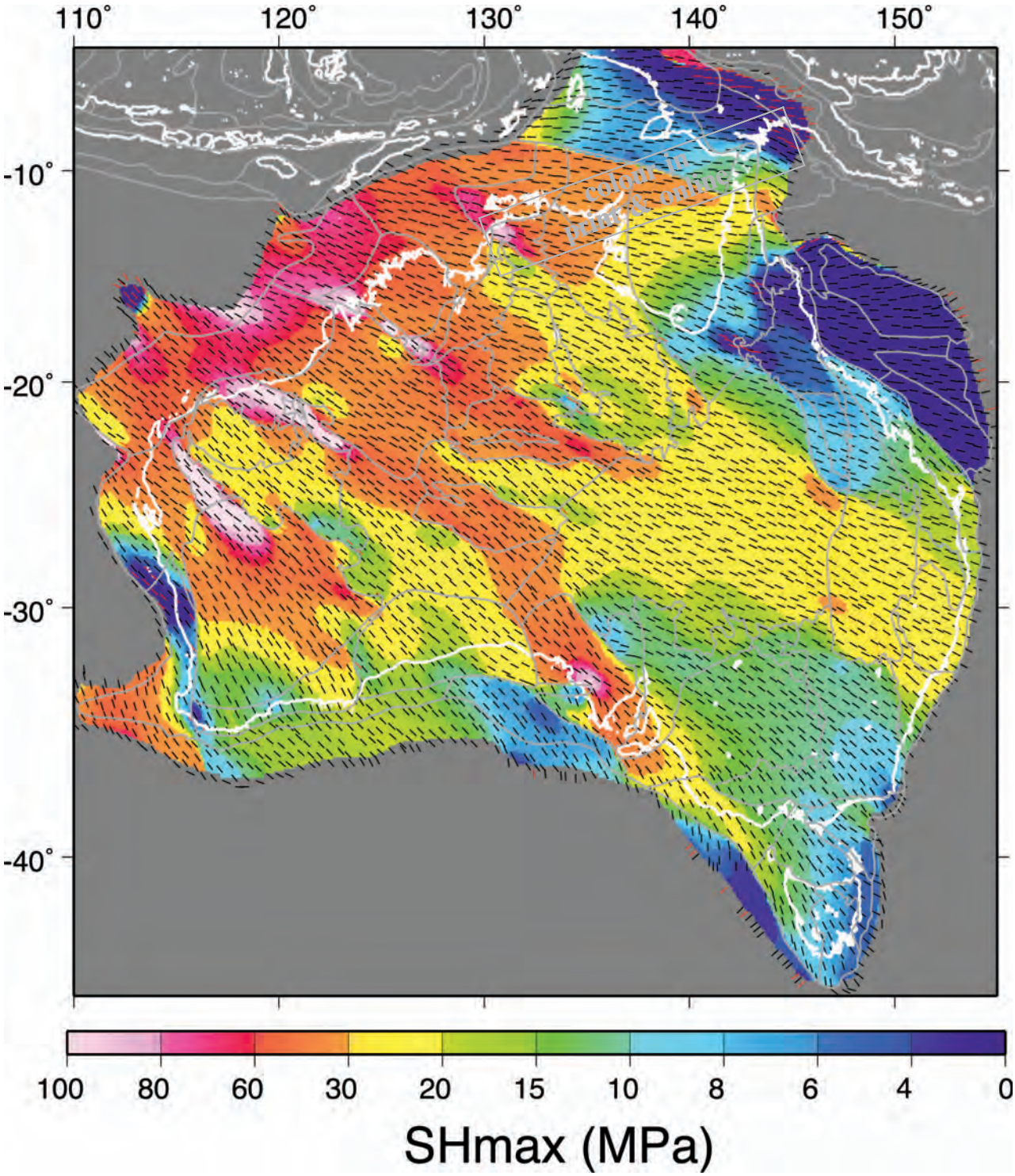

Figure 11 Modelled maximum horizontal stress for the Early to Middle Miocene (23–11 Ma). Stress magnitude units are in MPa.

Modelled σ_H orientations in the Flinders Ranges during the Middle to Late Miocene show increased variability compared with previous time periods. Modelled σ_H directions were oriented roughly north–south over the Mt Lofty Ranges in the southern Adelaide Fold Belt at this time and roughly east–west over the Flinders Ranges toward the north. Conditions favourable for reverse reactivation along the Flinders Ranges were re-established in the Middle to Late Miocene and reverse reactivation of moderately dipping, north–south-trending range bounding faults in the Flinders Ranges was likely at this time (Figure 3B3), potentially triggering the second, ongoing phase of the Sprigg's Orogeny (Dyksterhuis & Müller 2008). Based on observations from the Simpson Desert, Sprigg (1963) estimated that basin (and gentle

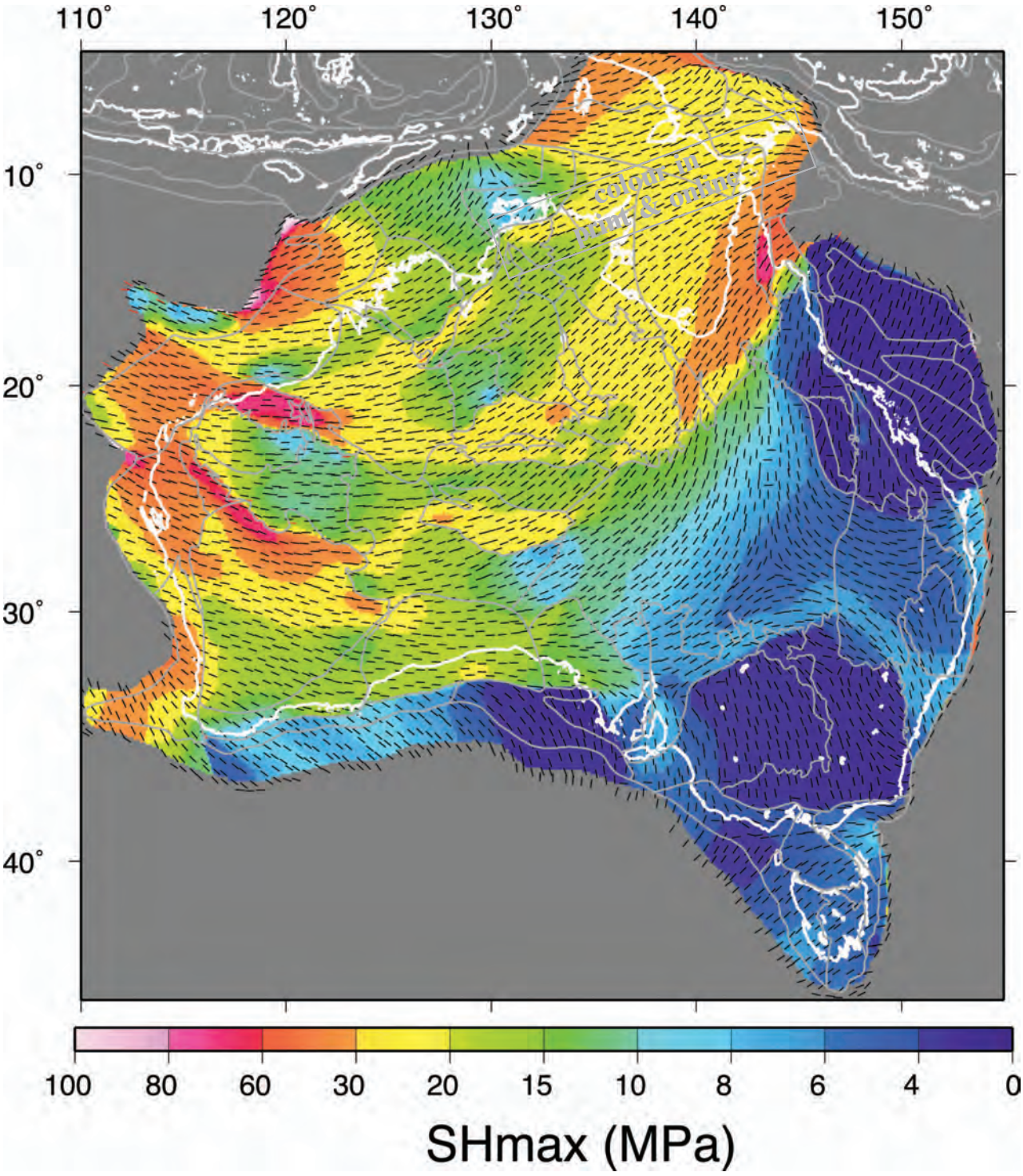

Figure 12 Modelled maximum horizontal stress for the Late Miocene (11–6 Ma). Stress magnitude units are in MPa.

syncline) formation, coincident with Simpson Desert depression, has continued during the Neogene in the southwestern Eromanga Basin. This is compatible with our model results. Modelled σ_H directions in the Gippsland Basin rotate to an east–west orientation in the Middle to Late Miocene and a reverse stress regime existed. Reactivation of east–west-trending, steeply dipping faults is interpreted as unlikely at this time (Figure 3C3).

CONTEMPORARY (6–0 MA)

Convergence speed along the southern portion of the Pacific–Australia plate boundary increased twofold at about 6 Ma (Cande & Stock 2004) (Figure 2D). Changes in compressional forces along the New Zealand margin between the Middle Miocene and present day do not greatly effect the modelled σ_H regime over the NWS, with present day modelled σ_H directions and magnitudes

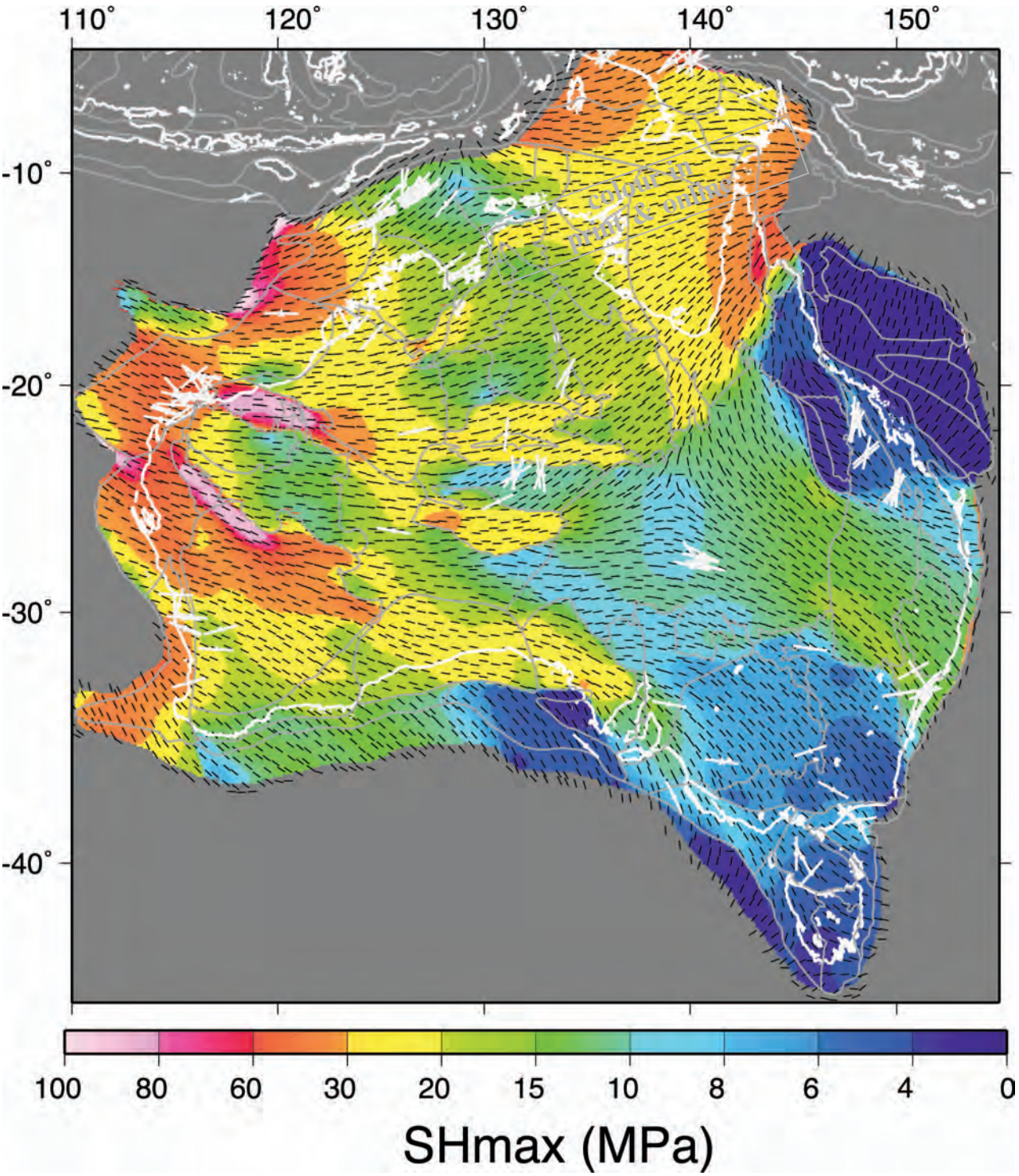

Figure 13 Modelled contemporary (6–0 Ma) maximum horizontal stress. Orientation data from the Australian Stress Map Database shown by white filled bars. Stress magnitude units are in MPa.

(Figure 13) similar to those in the Middle–Late Miocene. Transpressional reactivation of northeast-trending steeply dipping faults in the Browse Basin is likely based on slip tendency analysis (Figure 3A4).

Modelled σ_H magnitudes over the Flinders Ranges increase in response to increased convergence along the southeast margin of the Indo-Australian Plate. Reverse reactivation of moderately dipping, north–south-trending range bounding faults in the Flinders Ranges is still likely at this time (Figure 3B4). High Quaternary slip rates on range bounding faults showing reverse sense motion in the Flinders Ranges (Sandiford 2003) demonstrate evidence for this modelled σ_H regime.

Modelled present-day σ_H directions in the Gippsland Basin trend northwest and agree with observed northwest-trending σ_H orientations (Hillis & Reynolds 2000). Modelled σ_H directions and magnitudes indicate that reverse reactivation is likely (Figure 3C4) and are

supported by observations of continued growth on north-east-trending anticlines in the region into the Pliocene. Dickinson *et al.* (2001) observed that up to one kilometre of exhumation or more has occurred in the Gippsland and Otway Basins post Middle Miocene.

CONCLUSIONS

Our models indicate that significant changes in the stress regime of the geologically heterogeneous Australian continent through time can be modelled by changing geometry and forces acting along the boundaries of the Indo-Australia and Paleo-Australian plate since the Early Cretaceous and we demonstrate that intraplate structural events may be caused by interaction of the far field stress field with the heterogeneous geology of Australia. We validate our paleo-stress models by examining the fault reactivation histories of various sedimentary basins in Australia. Our modelling indicates that intraplate suture zones of the Australian continent that were particularly weak, such as the strongly faulted portions of the Northwest Shelf and the Flinders Ranges, have been reactivated during times when favourable stress regimes existed. Our modelling approach, which includes spatial variations in plate stiffness, clearly supports the hypothesis that pre-existing weaknesses in continental crust can act to localise deformation, and we show quantitatively how juxtaposed strengths and weaknesses in the plate together with time-varying plate driving forces act to reactivate particular portions of the continental crust with tectonic fabric orientations favourable for reactivation through time. Our models provide a tectonic framework, validated with geological observations, for understanding first-order structural reactivation of the Australian continent and shelf. The digital paleo-stress models discussed in this paper are accessible at http://www.earthbyte.org.

ACKNOWLEDGEMENTS

We thank Judith Sippel and Alexey Goncharov for their constructive reviews that improved the paper substantially. RDM was supported by ARC FL0992245 and PR by ARC grant DP0987604.

REFERENCES

Aitchison J., Ali J. R. & Davis A. M. 2007. When and where did India and Asia collide? *Journal of Geophysical Research* **112**, doi:10.1029/2006JB004706.

Alexander E. M. & Jensen-Schmidt B. 1996. Structural and tectonic history. *Department of Mines and Energy. The Petroleum Geology of South Australia.*

Alley N. F. 1998. Cainozoic stratigraphy, palaeoenvironments and geological evolution of the Lake Eyre Basin. *Palaeogeography, Palaeoclimatology, Palaeoecology* **144**, 239–263.

Baillie P. W. & Jacobson E. 1995. Structural evolution of the Carnarvon Terrace, Western Australia. *The APEA Journal* **35**, 321–332.

Bernecker T., Thomas J. H. & O'Brien G. W. 2006. *Hydrocarbon prospectivity of areas V06-2, V06-3 and V06-4, southern offshore Gippsland Basin, Victoria, Australia.* Industries V. D. o. P.

Brun J. P. & Nalpas T. 1996. Graben inversion in nature and experiments. *Tectonics* **15**, 677–687.

Cande S. C. & Stock J. M. 2004. Pacific–Antarctic–Australia motion and the formation of the Macquarie plate. *Geophysical Journal International* **157**, 399–414.

Celerier J., Sandiford M., Hansen D. L. & Quigley M. 2005. Modes of active intraplate deformation, Flinders Ranges, Australia. *Tectonics* **24**, C6006–C6006.

Clark D. & Leonard M. 2003. Principal stress orientations from multiple focal-plane solutions: new insight into the Australian intraplate stress field. *In*: Hillis R. R. & Müller D. eds. *Evolution and dynamics of the Australian Plate*, Vol. 22, p. 438, Geological Society of Australia Special Publication, Sydney.

Cloetingh S., Stein C., Reemst P., Gradstein F., Williamson P., Exon N. & von Rad U. 1992. Continental margin stratigraphy, deformation, and intraplate stresses for the Indo-Australian region. *In*: Gradstein F. M., Ludden J. N. *et al.* eds. *Proceedings of the Ocean Drilling Program, scientific results, Vol. 123*, pp. 671–713.

Dickinson J. A., Wallace M. W., Holdgate G., Daniels J., Gallagher S. J. & Thomas L. 2001. Neogene tectonics in SE Australia: Implications for Petroleum Systems. *APPEA Journal* **41**, 37–51.

Dyksterhuis S. & Müller D. 2004. Modelling the contemporary and palaeo stress field of Australia using finite-element modelling with automatic optimisation. *Exploration Geophysics* **35**, 236–241.

Dyksterhuis S. & Müller R. D. 2008. Cause and evolution of intraplate orogeny in Australia. *Geology* **36**, 495–498.

Dyksterhuis S., Albert R. A. & Müller D. 2005a. Finite element modelling of intraplate stress using ABAQUS™. *Journal of Computers and Geosciences* **31**, 297–307.

Dyksterhuis S., Müller R. D. & Albert R. A. 2005b. Palaeo-stress field evolution of the Australian continent since the Eocene. *Journal of Geophysical Research* **110**, B05102 doi:05110.01029/02003JB002728.

Etheridge M., McQueen H. & Lambeck K. 1991. The role of intraplate stress in Tertiary (and Mesozoic) deformation of the Australian continent and its margins: A key factor in petroleum trap formation. *Exploration Geophysics* **22**, 123–128.

Finlayson D. M. & Leven J. H. 1988. Structural Styles and Basin Evolution in Eromanga Region, Eastern Australia. *American Association of Petroleum Geologists* **72.**

Gaina C. & Müller R. D. 2007. Cenozoic tectonic and depth/age evolution of the Indonesian gateway and associated back-arc basins. *Earth Science Reviews* **83**, 177–203.

Gibson P. J. 1989. Petrology of two Tertiary oil shale deposits from Queensland, Australia. *Journal of the Geological Society of London* **146**, 319–331.

Glen R. A. & Brown R. E. 1993. A transect through a forearc basin: preliminary results from a transect across the Tamworth Belt at Manilla N.S.W., *In*: Flood P. G. & Aitchison J. C. eds. New England Orogen, eastern Australia: Armidale, Department of Geology & Geophysics, University of New England, 105–111.

Gregory C. M., Senior B. R. & Galloway M. C. 1967. The geology of the Connemara, Jundah, Canterbury, Windorah and Adavale 1:250,000 shet areas, Queensland. *Bureau of Mineral Resources.*

Hall R. 2002. Cenozoic geological and plate tectonic evolution of SE Asia and the SW Pacific: computer-based reconstructions, model and animations. *Journal of Asian Earth Sciences* **20**, 353–431.

Heidbach O., Reinecker J., Tingay M., Müller B., Sperner B., Fuchs K. & Wenzel F. 2007. Plate boundary forces are not enough: Second- and third-order stress patterns highlighted in the World Stress Map database. *Tectonics* **26**, doi:10.1029/2007TC002133.

Hill P. J. 1994. Geology and geophysics of the offshore Maryborough, Capricorn and northern Tasman Basins. *AGSO Australian Geological Survey Organisation Record.*

Hillis R. R. & Reynolds S. D. 2000. The Australian stress map. *Journal of the Geological Society of London* **157**, 915–921.

Hobbs B. E. 1985. Interpretation and analysis of structure in the Bowen Basin (unpubl.).

Johnstone R. D., Jenkins C. C. & Moore M. A. 2001. An integrated structural and palaeogeographic investigation of Eocene erosional events and related hydrocarbon potential in the Gippsland Basin. *Eastern Australasian Basins Symposium 2001*, Melbourne, pp. 403–412. The Australasian Institute of Mining and Metallurgy.

KAMP P. J. J. & FITZGERALD P. G. 1987. Geologic constraints on the Cenozoic Antarctica–Australia–Pacific relative plate motion circuit. *Geology* **15**, 694–697.

KEEP M., POWELL C. McA. & BAILLIE P. W. 1998. Neogene Deformation of the North West Shelf, Australia. *The Sedimentary Basins of Western Australia 2.* Perth, Australia, pp. 81–94. Petroleum Exploration Society of Australia.

KORSCH R. J., TOTTERDELL J. M., FOMIN T. & NICOLL M. G. 2009. Contractional structures and deformational events in the Bowen, Gunnedah and Surat Basins, eastern Australia. *Australian Journal of Earth Sciences* **56**, 477–499.

KRISHNA K. S., RAO D. G., RAMANA M. V., SUBRAHMANYAM V., SARMA K. V. L. N. S., PILIPENKO A. I., SHCHERBAKOV V. S. and RADHAKRISHNA MURTHY I. V. 1995. Tectonic model for the evolution of oceanic crust in the northeastern Indian Ocean from the Late Cretaceous to the early Tertiary. *Journal of Geophysical Research* **100**, 20011–20024.

LONGLEY I. M., BUESSENSCHUETT C., CLYDESDALE L., CUBITT C. J., DAVIS R. C., JOHNSON M. K., MARSHALL N. M., SOMERVILLE R., SPRY T. B. & THOMPSON N. B. 2002. The North West Shelf of Australia—a Woodside perspective. *In*: Keep M. & Moss S. J. eds. *The sedimentary basins of Western Australia 3*, pp. 27–86, Petroleum Exploration Society of Australia, Perth, WA.

MATTHEWS K. J., HALE A. J., GURNIS M., MÜLLER R. D. & DICAPRIO L. 2011. Dynamic subsidence of Eastern Australia during the Cretaceous. *Gondwana Research* **19**, 372–383.

MAVROMATIDIS A. 2006. Burial/exhumation histories for the Cooper Eromanga Basins and implications for hydrocarbon exploration, Eastern Australia. *Basin Research* **18**, 351–373.

MCCONNOCHIE M. J. & HENSTRIDGE D. A. 1985. The Lowmead Graben—geology, Tertiary oil shale genesis and regional tectonic implications. *Australian Journal of Earth Sciences* **32**, 205–218.

MITCHELL M. M., KOHN B. P., O'SULLIVAN P. B., HARTLEY M. J. & FOSTER D. A. 2002. Low-temperature thermochronology of the Mt Painter Province, South Australia. *Australian Journal of Earth Sciences* **49**, 551–563.

MORRIS A., FERRILL D. A. & HENDERSON D. B. 1996. Slip-tendency analysis and fault reactivation. *Geology* **24**, 275–278.

MÜLLER D., MIHUT D., HEINE C., O'NEIL C. & RUSSELL I. 2002. Tectonic and volcanic history of the Canarvon Terrace: Constraints from seismic interpretation and geodynamic modelling. *The Sedimentary Basins of Western Australia 3*, Perth, Western Australia, pp. 719–740. Petroleum Exploration Society of Australia.

O'BRIAN G. W., LISK M., DUDDY I., EADINGTON P. J., CADMAN S. & FELLOWS M. 1996. Late Tertiary fluid migration in the Timor Sea: A key control on thermal and diagenetic histories? *APEA Journal* **1996**, 399–426.

QUIGLEY M. C., CUPPER M. L. & SANDIFORD M. 2006. Quaternary faults of south-central Australia: palaeoseismicity, slip rates and origin. *Australian Journal of Earth Sciences* **53**, 285–301.

REY P. F. & MÜLLER R. D. 2010. Fragmentation of active continental margins owing to the buoyancy of the mantle wedge. *Nature Geoscience* **3**, 257–261.

ROYER J-Y. & CHANG T. 1991. Evidence for relative motions between the Indian and Australian plates during the last 20 m.y. from plate tectonic reconstructions: implications for the deformation of the Indo-Australian plate. *Journal of Geophysical Research* **96**, 11779–11802.

SANDIFORD M. 2003. Neotectonics of southeastern Australia: linking the Quaternary faulting record with seismicity and in situ stress. *In*: Hillis R. R. & Müller D. eds., *Evolution and dynamics of the Australian Plate*, Vol. 22, p. 438, Geological Society of Australia Special Publication, Sydney.

SANDIFORD M., WALLACE M. & COBLENTZ D. 2004. Origin of the in situ stress field in south-eastern Australia. *Basin Research* **16**, 325–338.

SENIOR B. R., GALLOWAY M. C., INGRAM J. A. & SENIOR D. 1968. The geology of the Barrolka, Eromanga, Durham Downs, Thargomindah, Tickalara and Bulloo 1:250,000 Sheet areas, Queensland. *Bureau of Mineral Resources*.

SHUSTER M. W., EATON S., WAKEFIELD L. L. & KLOOSTERMAN H. J. 1998. Neogene tectonics, greater Timor Sea, offshore Australia: Implications for trap risk. *The APPEA Journal* **38**, 351–379.

SPRIGG R. C. 1963. Geology and Petroleum prospects of the Simpson Desert. *Transactions of the Royal Society of South Australia* **86**, 36–65.

SPRIGG R. C. 1986. The Eromanga Basin in the search for commercial hydrocarbons. *In*: Gravestock D. I., Moore P. S. & Pitt G. M. eds., *Contributions to the geology and hydrocarbon potential of the Eromanga Basin*, Vol. Special Publ. 12, pp. 9–24, Geol. Soc. Aust., Sydney.

STRUCKMEYER H. I. M., BLEVIN J. E., SAYERS J., TOTTERDELL J. M., BAXTER K. & CATHRO D. L. 1998. Structural evolution of the Browse basin, North West Shelf: new concepts from deep-seismic data. *The sedimetary basins of Western Australia 2: Proceedings of Petroleum Exploration Society of Australia Symposium*, Perth, WA, pp. 345–367. Petroleum Exploration Society of Australia.

SYMONDS P. A. & CAMERON P. J. 1977. The structure and stratigraphy of the Carnarvon Terrace and Wallaby Plateau. *APEA Journal* **17**, 30–41.

SYMONDS P. A., COLLINS C. D. N. & BRADSHAW J. 1994. Deep structure of the Browse Basin: implications for basin development and petroleum exploration. *The Sedimentary Basins of Western Australia. Proceedings of the Petroleum Exploration Society of Australia, Perth* 315–332.

TULLOCH A. J., BEGGS M., KULA J. L., SPELL T. L. & MORTIMER N. 2006. Cordillera Zealandia, the Sisters Shear Zone and their influence on the early development of the Great South Basin, New Zealand. *New Zealand Petroleum Conference*, New Zealand. Ministry of Economic Development.

WOODWARD N. B. 1995. Thrust systems in the Tamworth Zone, southern New England Orogen, New South Wales. *Australian Journal of Earth Sciences* **42**, 107–117.

WOPFNER H. 1974. Post-Eocene History and Stratigraphy of Northeastern South Australia. *Transactions of the Royal Society of South Australia* **98**, 1–12.

WOPFNER H. 1978. Silcretes of northern South Australia and adjacent regions. *In*: Langford-Smith T. ed., *Silcrete in Australia.* pp. 93–141, Department of Geography, University of New England, Armidale.

ZOBACK M. 1992. First- and second-order patterns of stress in the lithosphere: the World Stress Map Project. *Journal of Geophysical Research* **97**, 11,703–11,728.

Received 2 February 2011; accepted 13 July 2011

APPENDIX 1 PROJECTION PARAMETERS

Listed here are the projections used for transforming points of latitude and longitude along the plate margins to and from a Cartesian reference frame for use in ABAQUS.

CONTEMPORARY
Lambert conical conformal projection with an origin of 132°E longitude, 25°S latitude and parallels at 15°S and 35°S

MIOCENE
Lambert conical conformal projection with an origin of 130°E longitude, 37°S latitude and parallels at 0°S and 40°S

EOCENE
Lambert conical conformal projection with an origin of 132.5°E longitude, 50°S latitude and parallels at 20°S and 50°S

CRETACEOUS
Lambert conical conformal projection with an origin of 120°E longitude, 50°S latitude and parallels at 40°S and 60°S.